



Optimisation of CdS–TCO bilayers for their application as windows in photovoltaic solar cells

M.A. Martínez^{*}, C. Guillén, M.T. Gutiérrez, J. Herrero

Instituto de Energías Renovables (CIEMAT), Avda. Complutense 22, E-28040 Madrid, Spain

Received 31 July 1995; revised 15 December 1995; accepted 15 March 1996

Abstract

The influence of CdS thickness and TCO deposition condition on the optoelectronic, morphological and structural properties of CdS–TCO bilayers has been studied. CdS was deposited by chemical bath, whereas the TCOs (ITO and aluminium-doped ZnO) were prepared by rf-magnetron sputtering. Cadmium sulphide thicknesses below 0.1 μm have been found to be optimal for avoiding optical absorption losses and conductivity deterioration. Though both types of window coatings, with TCO made at 25 and 200°C, have good quality, the ITO-based samples have shown a higher infrared transmission than those based on ZnO. Additionally, 10 and 70 minutes air-annealing treatments at 200°C have been carried out. Their analysis has demonstrated that the shorter ones are more suitable for enhancing crystalline structure maintaining unchanged electro-optical characteristics.

Keywords: Cadmium sulfide; Indium tin oxide; Semiconductor thin films; Thin film solar cells; Zinc oxide

1. Introduction

Both high conductivity and high transparency are required for solar-cell window layers. Cadmium sulphide, CdS, is known as a very suitable window layer in solar cells such as those based on CdTe [1] or CuInSe₂ [2]. The energy gap of the CdS is near the photon energy of the solar spectrum maximum, however, CdS films are prepared as thin as possible by film deposition techniques such as chemical bath deposition (CBD) [3], sputtering [4], screen-printing [5], spray pyrolysis [6], evaporation [7]... in order to avoid optical absorption losses.

Considering the application of these coatings to photovoltaic solar cells, the use of an

^{*} Corresponding author. Fax: 34 1 3466037.

additional transparent conductive oxide (TCO) film is necessary in order to compensate the sheet resistance of the cadmium sulphide [8]. Accordingly, the CuInSe₂ and CdTe window layers are a combination of two thin films, a cadmium sulphide film and a TCO front contact. Both are wide bandgap semiconductors and the optimisation of the optoelectronic features of either of them contributes to improve solar-cell performance.

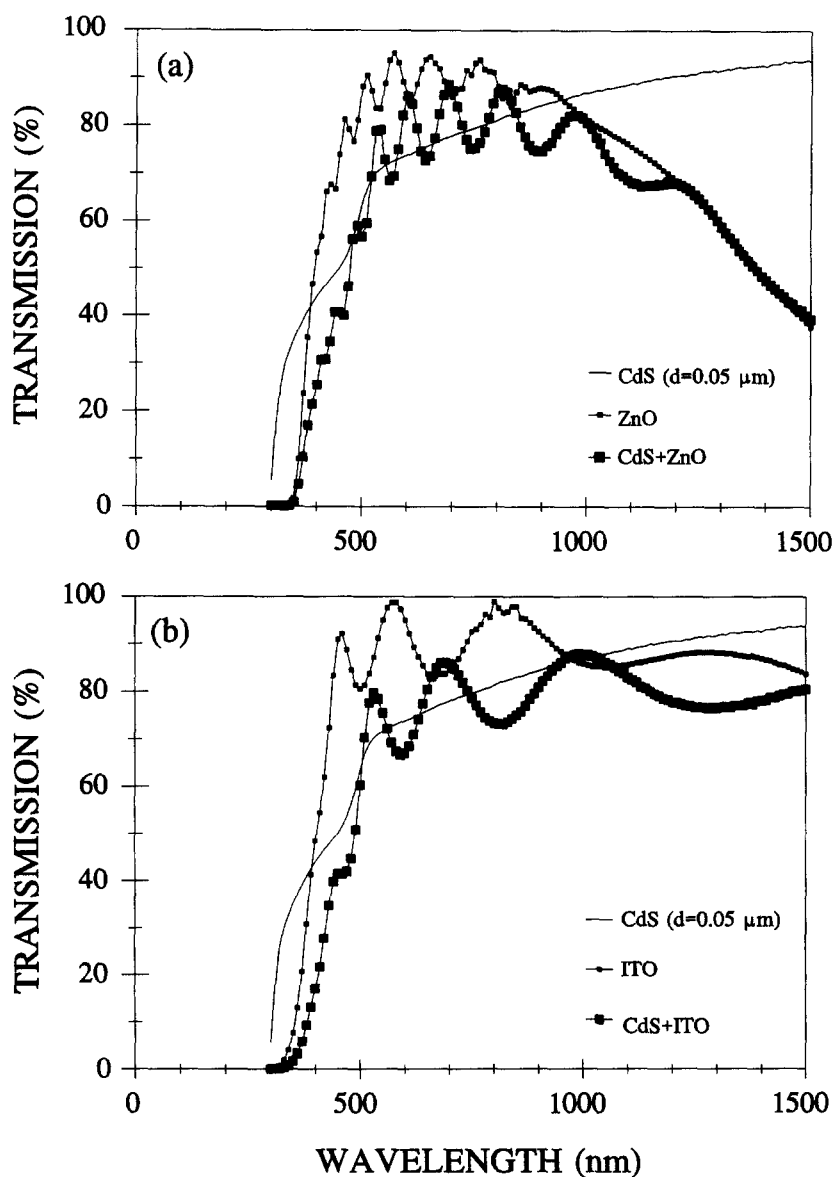


Fig. 1. Optical transmission spectra of CdS-TCO bilayers with $d_{\text{CdS}} = 0.05 \mu\text{m}$ and (a) ZnO or (b) ITO. The TCO preparation temperature is 25°C.

The investigation of combined CdS–TCO films has recently been developed owing to the great interest of better understanding the effect of these bilayers on the absorbers [9,10]. Taking into account the importance of such window coatings, the present work reports on the analysis of the optoelectronic, structural and morphological properties of bilayers consisting of rf-magnetron sputtered indium tin oxide or aluminium-doped zinc oxide and chemical bath deposited cadmium sulphide. The research has been focused on the optimisation of the CdS thickness, the TCO optoelectronic behaviour and the structural coupling between both materials.

2. Experimental procedure

The cadmium sulphide coatings have been made on Tempax glass substrates at 60°C by chemical bath deposition in the standard conditions published elsewhere [11,12]. The deposition time has been the only preparation parameter ranged, in order to obtain different thicknesses, d . Subsequently, indium tin oxide, ITO, or aluminium-doped zinc oxide, ZnO, has been deposited by means of a commercial rf-magnetron sputtering system (Leybold Heraeus Z-400). For this purpose two different targets have been supplied by Cerac Inc.: $\text{In}_2\text{O}_3\text{:SnO}_2$ 95/5 wt% 99.99 purity and $\text{ZnO:Al}_2\text{O}_3$ 98/2 wt% 99.99 purity. The argon and oxygen mass-flow rates, presputtering and sputtering times, rf-power density and base pressure have been selected from our previous investigations [13–15]. The preparation sequence chosen, first CdS and secondly TCO, is the most usual window layer configuration in CuInSe_2 -based photovoltaic solar cells. The glass + CdS substrate temperature has not been raised above 200°C, because it is well known that the CdS– CuInSe_2 interface deteriorates at higher temperatures [16,17]. Taking into account that the CuInSe_2 -based solar cell efficiency sharply enhances by heating the

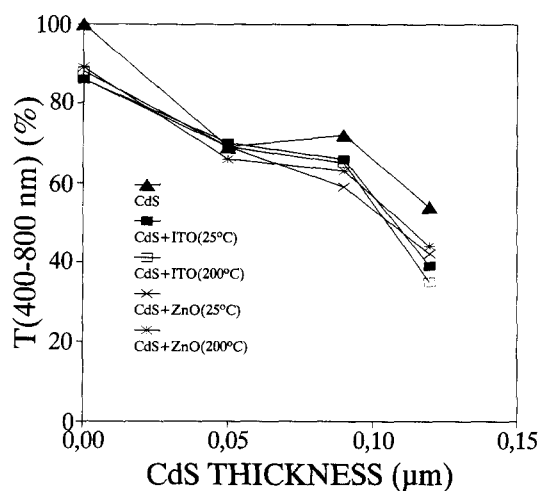


Fig. 2. Evolution of the average transmission in the 400–800 nm wavelength range with the CdS thickness, for samples made using different deposition conditions.

device in air for short times at 200°C [2], but not much more for long times [17], the as-grown CdS–ITO and CdS–ZnO samples made at room temperature have been annealed in air at 200°C for 10 and 70 minutes in a tubular furnace in order to test and compare their evolution.

The thicknesses of the films have been estimated independently by utilising a Dektak 3030 surface profile measurement unit and by interference in the near-infrared transmission spectra [18]. Optical transmission, T , measurements have been done at room temperature with unpolarized light at normal incidence in the wavelength range from 300 to 2500 nm, with a double-beam spectrophotometer (Perkin Elmer Lambda 9). The combined CdS–TCO film resistances have been determined by means of a four point probe system (Veeco model FPP5000) and the structural and morphological properties have been deduced from X-ray diffraction, electron diffraction and TEM measurements (Phillips Electronics Inc. PW1370 diffractometer and JEOL JEM 2000FX Electron Microscope, respectively).

3. Results and discussion

3.1. As-grown films

The first set of samples has been made with the ITO and ZnO both prepared at 25 and 200°C on cadmium sulphide films of thicknesses varying between 0.05 and 0.12

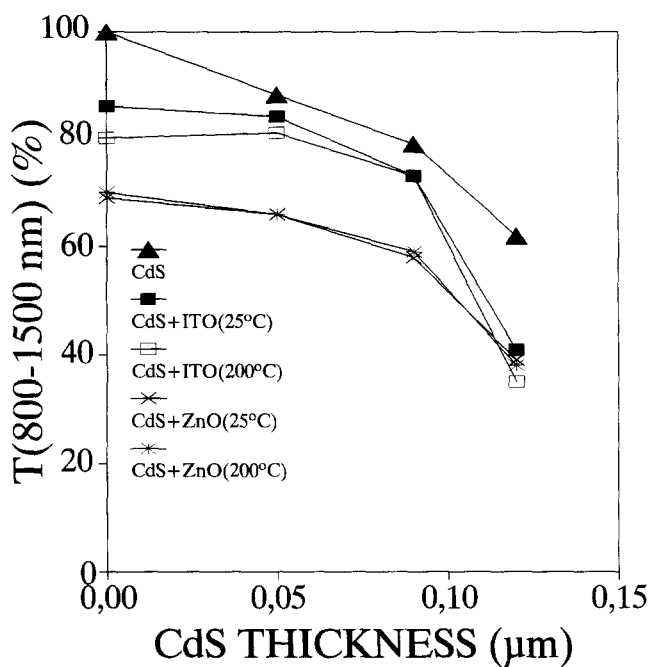


Fig. 3. Variation of the infrared average transmission with the CdS thickness for bilayers deposited using different conditions.

μm . Variations in TCO processing have been neglected owing to the reproducibility and reliability demonstrated in previous studies [13–15]. In all cases TCO and CdS data have been taken as references for the corresponding bilayers.

Typical transmission spectra can be observed in Fig. 1a and 1b for coatings prepared at room temperature with the thinnest CdS. From them, no significant differences between ITO and ZnO can be established in the visible range, because both materials are very transparent, $T = 80\text{--}90\%$, in this zone. The only differences are associated with the interferences produced by their different thicknesses [18], $0.5\ \mu\text{m}$ for ITO and $0.8\text{--}0.9\ \mu\text{m}$ for ZnO. Such thicknesses are the best for obtaining the appropriate optoelectronic quality [13–15]. These spectra have been analyzed in two different intervals: visible ($400\text{--}800\ \text{nm}$) and infrared ($800\text{--}1500\ \text{nm}$), in order to evaluate the influence of CdS and TCO on each region. It has been proved that average transmittances in the $400\text{--}800\ \text{nm}$ wavelength range are mainly dependent on the cadmium sulphide thickness [10], decreasing for increasing thicknesses, Fig. 2, as a consequence of the higher absorption in the CdS. Nevertheless, for a given cadmium sulphide thickness, T remains relatively constant even if both the deposition conditions and the sputtering target used for preparing the TCO have been changed.

Likewise, the behaviour of the average transmittances in the $800\text{--}1500\ \text{nm}$ wavelength range has been checked. Looking again at Fig. 1, the influence of the ITO and ZnO on this interval can be appreciated. Aluminium-doped zinc oxide shows a sharper reduction of T in the infrared region than ITO, due to the higher rf-power densities

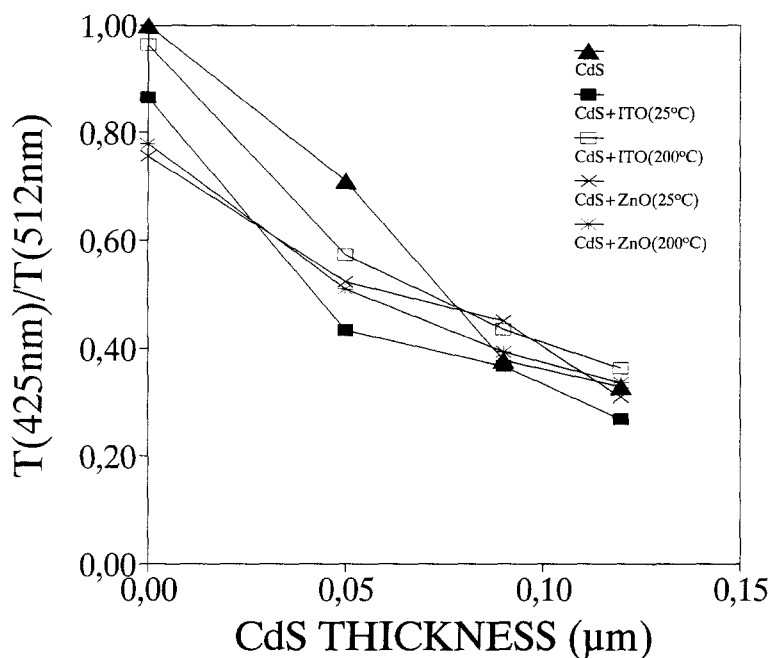


Fig. 4. Influence of the cadmium sulphide thickness on the $T_{425\text{nm}}/T_{512\text{nm}}$ ratio for films made with different sputtering targets at 25 and 200°C substrate temperature.

needed for preparing the ZnO. In previous papers [13–15], it has been demonstrated that the utilisation of higher rf-power densities creates a great number of oxygen vacancies and, therefore, a high quasi-free carrier concentration. Thereby, the absorption of the quasi-free electrons raises and the global effect on the transmission spectra is a reduction in the infrared zone.

In Fig. 3 the variation of T in the 800–1500 nm region with the cadmium sulphide thickness has been represented. CdS–ITO bilayer results are better for all thicknesses used except for the thickest CdS. It seems that the TCO growth can be affected by the powdery CdS surfaces obtained when $d_{\text{CdS}} = 0.12 \mu\text{m}$. Such powdery and yellowish appearances have been attributed to the adhesion of solution particles on the CdS thin film surface during the CBD process [19]. Since these solution particles grow simultaneously to the CdS thin film, increasing their amount and size with the deposition time, the thickest CdS layers are more powdery and yellowish.

In order to compare the transmission losses, the ratio of film transmission at certain wavelengths has been compared for the different deposition conditions. The closer the value is to one, the lower the amount of absorption and the better the transmission [9,10]. In the short wavelength region, the ratio taken is $T_{425\text{nm}}/T_{512\text{nm}}$ and in the long wavelength region the ratio is $T_{1400\text{nm}}/T_{1200\text{nm}}$. The transmittance values of the samples have been compared in Figs. 4 and 5. From these data it has been seen that the

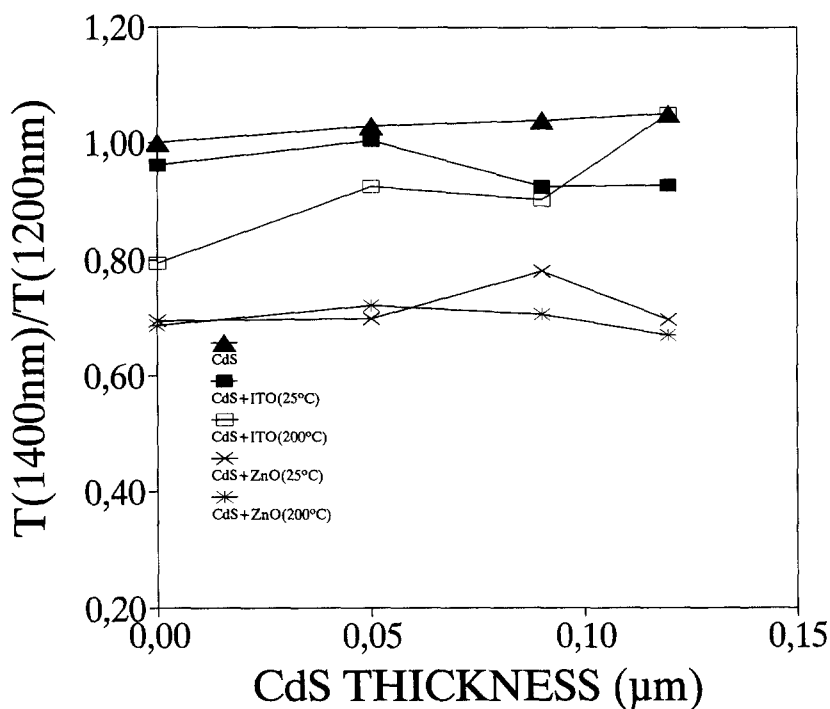


Fig. 5. Dependence of the $T_{1400\text{nm}}/T_{1200\text{nm}}$ ratio on the CdS thickness for samples prepared in different deposition conditions.

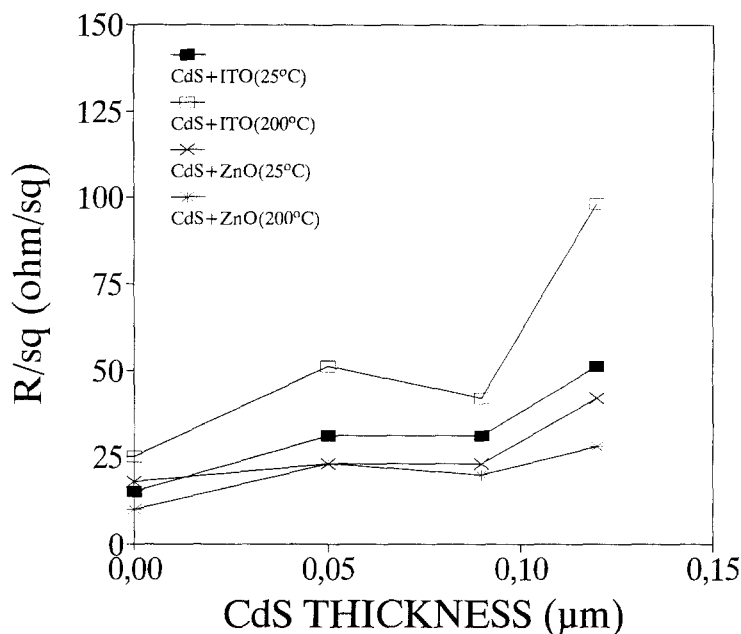


Fig. 6. Variation of sheet resistance with the cadmium sulphide thickness for bilayers deposited in different conditions.

$T_{425\text{nm}}/T_{512\text{nm}}$ ratio, Fig. 4, is controlled by the CdS thickness and is independent of the ITO or ZnO coating characteristics. As the CdS thickness increases, the short wavelength transmission ratio decreases, yet that at long wavelengths is relatively constant for a given cadmium sulphide thickness. In the long wavelength zone, the transmission is dominated by the long wavelength absorption due to the TCO. Here, the $T_{1400\text{nm}}/T_{1200\text{nm}}$ ratio, Fig. 5, does not vary with the CdS thickness but changes with the type of transparent conductive oxide. Indium tin oxide shows a better $T_{1400\text{nm}}/T_{1200\text{nm}}$ ratio owing to its lower quasi-free carrier absorption in this zone.

On the other hand, the electrical quality has been examined by measuring the sheet resistance, R/\square . The results obtained for the different samples have been plotted in Fig. 6. From this, a relatively smooth rise of R/\square with the increasing cadmium sulphide thickness can be detected. Only for the thickest CdS grown, sheet resistance data have presented a worsening. This is attributed to TCO growth process modification when the CdS substrate is very porous.

According to the previous discussion, CdS-ITO films made at room temperature have exhibited the best optoelectronic quality for $d_{\text{CdS}} < 0.1 \mu\text{m}$ and can be considered as adequate window layers for CuInSe₂ or CdTe-based photovoltaic solar cells [1,2], always taking into account that the final optimisation should be performed in conjunction with the corresponding absorber. Besides, the influence of small variations of T and R/\square on the photovoltaic efficiency will be given by the cell design. Owing to this fact, none of the analyzed bilayers should be discarded as a valid window layer although the

Table 1

Optoelectronic features of window layers consisting of 25°C-rf-magnetron sputtered ITO on chemical bath deposited CdS layers of different thicknesses. Effect of the 200°C air annealing time

d_{CdS} (μm)	Annealing	$T(400\text{--}800\text{nm})$	$T(800\text{--}1500\text{nm})$	$T_{425\text{nm}} / T_{512\text{nm}}$	$T_{1400\text{nm}} / T_{1200\text{nm}}$	R / \square (Ω / \square)
0	no	0.858	0.860	0.865	0.962	15
0.05	no	0.705	0.843	0.434	1.004	31
0.09	no	0.656	0.731	0.367	0.926	31
0.12	no	0.389	0.407	0.269	0.928	51
0	10 min	0.858	0.827	0.854	0.888	21
0.05	10 min	0.710	0.830	0.467	1.012	34
0.09	10 min	0.631	0.744	0.403	0.975	29
0.12	10 min	0.380	0.430	0.309	1.015	39
0	70 min	0.886	0.763	0.902	0.889	31
0.05	70 min	0.717	0.746	0.544	0.888	58
0.09	70 min	0.627	0.713	0.449	0.870	62
0.12	70 min	0.374	0.427	0.340	0.942	56

CdS–ITO films deposited at 25°C have been selected as optimal. A summary of their electro-optical features can be observed in Table 1.

X-ray and electron diffraction studies have revealed that both compounds forming the bilayers, CdS–ITO and CdS–ZnO, maintain their independent structures. Thereby,

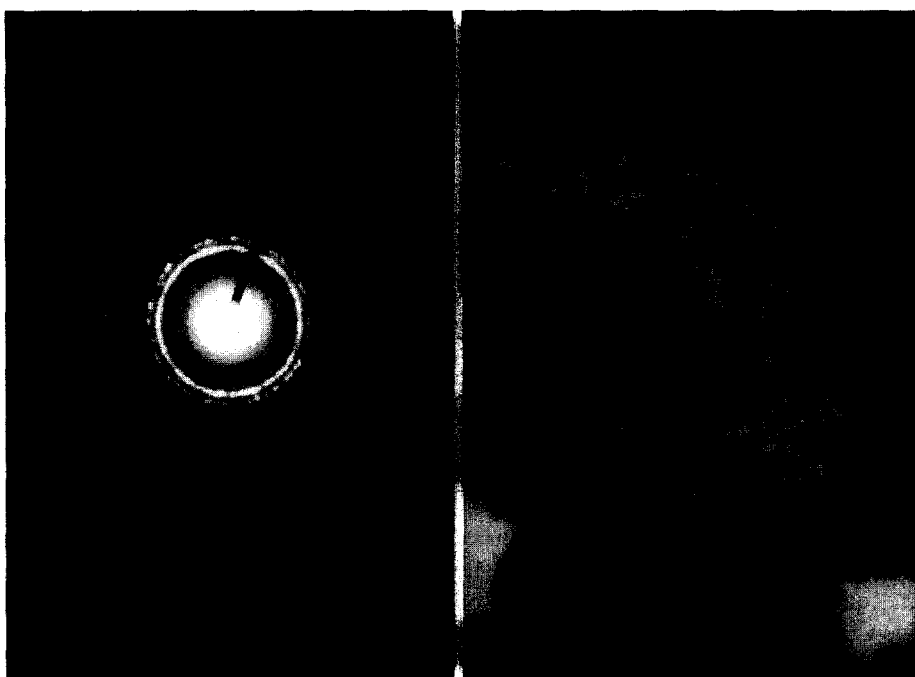


Fig. 7. (a) Electron diffraction pattern and (b) TEM photograph for a CdS–ZnO film made at room-temperature.

cadmium sulphide crystallises in the hexagonal system, presenting the (002) orientation as the preferred one [20]. ITO and ZnO in turn crystallise in the cubic [21] and hexagonal [22] systems, showing the (222) and (002) as their preferred orientations, respectively. Besides, their morphology has been evaluated by TEM, which has evidenced great differences in grain size corresponding with CdS or TCO. Fig. 7 illustrates

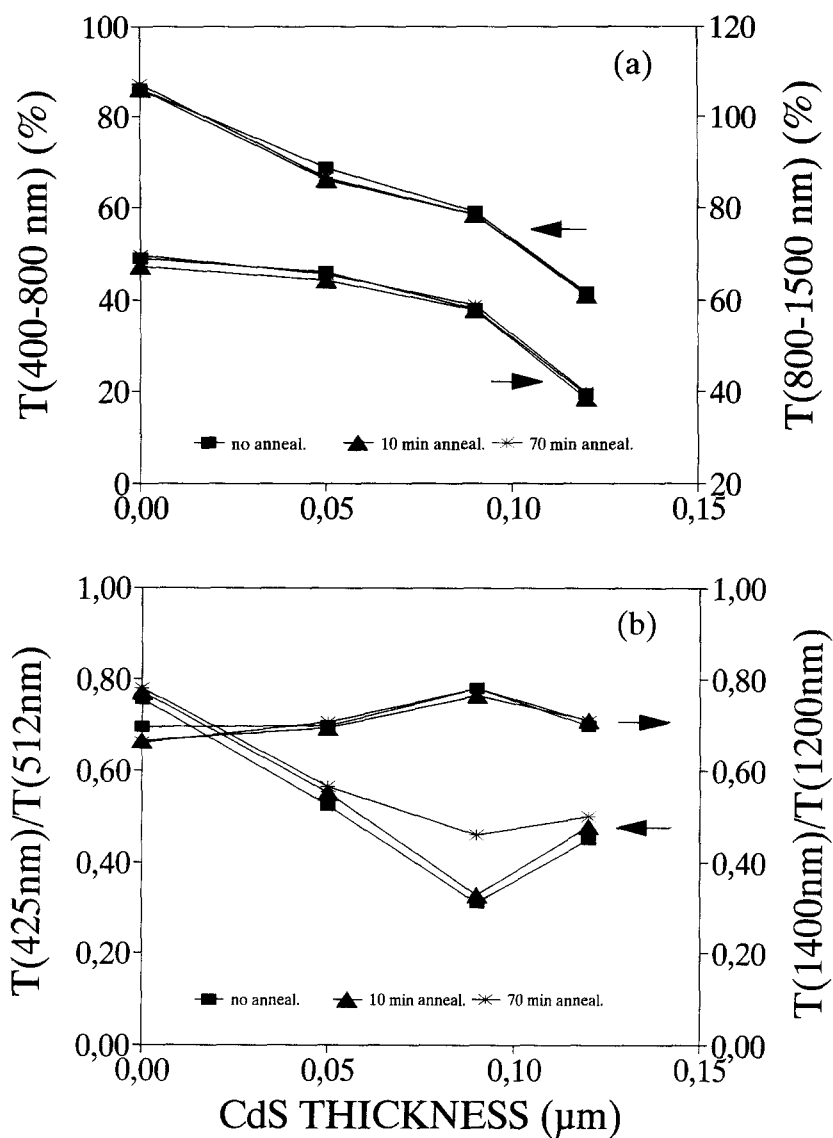


Fig. 8. Influence of the 200°C air annealing time on the (a) visible and infrared average transmissions and (b) $T_{425 \text{ nm}}/T_{512 \text{ nm}}$ and $T_{1400 \text{ nm}}/T_{1200 \text{ nm}}$ ratios for room-temperature ZnO films made on CdS layers of various thicknesses.

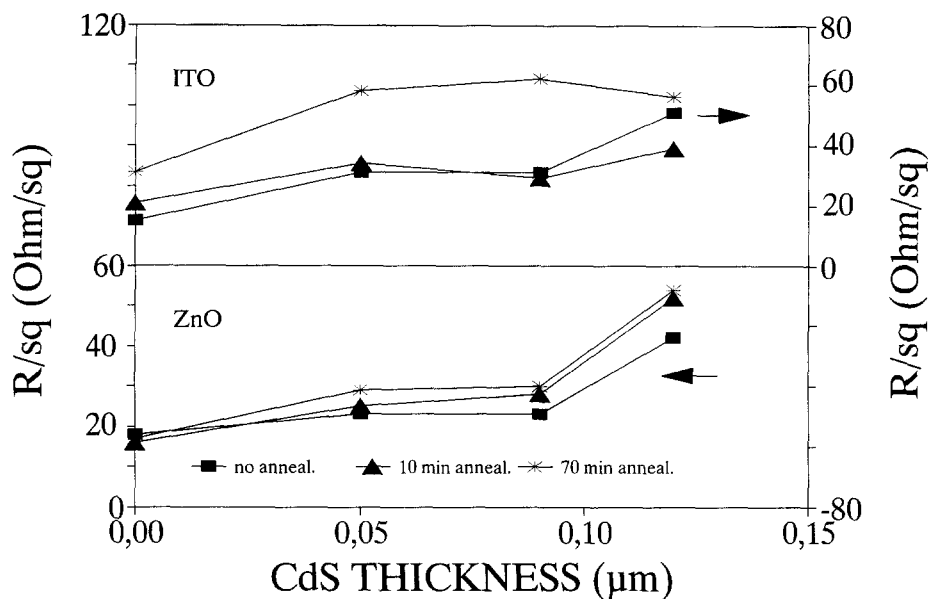


Fig. 9. Dependence of R/\square on the 200°C air annealing time for room-temperature TCO coatings deposited on CdS layers of several thicknesses.

the electron diffraction pattern (a) and the TEM image (b) belonging to a CdS + ZnO sample made at 25°C. The TEM photographs indicate that the CBD cadmium sulphide grains are one order of magnitude (~ 200 nm) larger than those of the rf-magnetron sputtered ZnO (~ 20 nm) when both layers, CdS and ZnO, have been prepared with similar thicknesses, ~ 0.1 μm . These grain sizes are typical of the corresponding materials made by such deposition methods. However, if solution particles have been adhered on the CdS thin film surface, the adhered particles sizes are observed to be some orders of magnitude larger.

3.2. Air-annealed films

Considering the efficiency enhancement reported for 200°C-air-annealed CuInSe₂-based solar cells [2], the next part of the work has been focused on the air-annealing at 200°C for 10 and 70 minutes of bilayers having the ITO and ZnO deposited at 25°C on CdS with $d_{\text{CdS}} = 0.05\text{--}0.12$ μm . In the ZnO case, see Figs. 8 and 9, it has been proved that the optoelectronic properties substantially remain unchanged in comparison with the as-grown films. Both CdS–ZnO average transmittances in the 400–800 nm and 800–1500 nm wavelength ranges (Fig. 8a) and the $T_{425\text{nm}}/T_{512\text{nm}}$ and $T_{1400\text{nm}}/T_{1200\text{nm}}$ ratios (Fig. 8b) have maintained good values for $d_{\text{CdS}} < 0.1$ μm . Additionally, the sheet resistance has not strongly worsened with the different air-heat treatments. Otherwise, the ITO is more sensitive to the oxygen incorporation to its crystalline lattice, especially during the longest air annealing treatment. Thus, the ITO sheet resistance has increased,

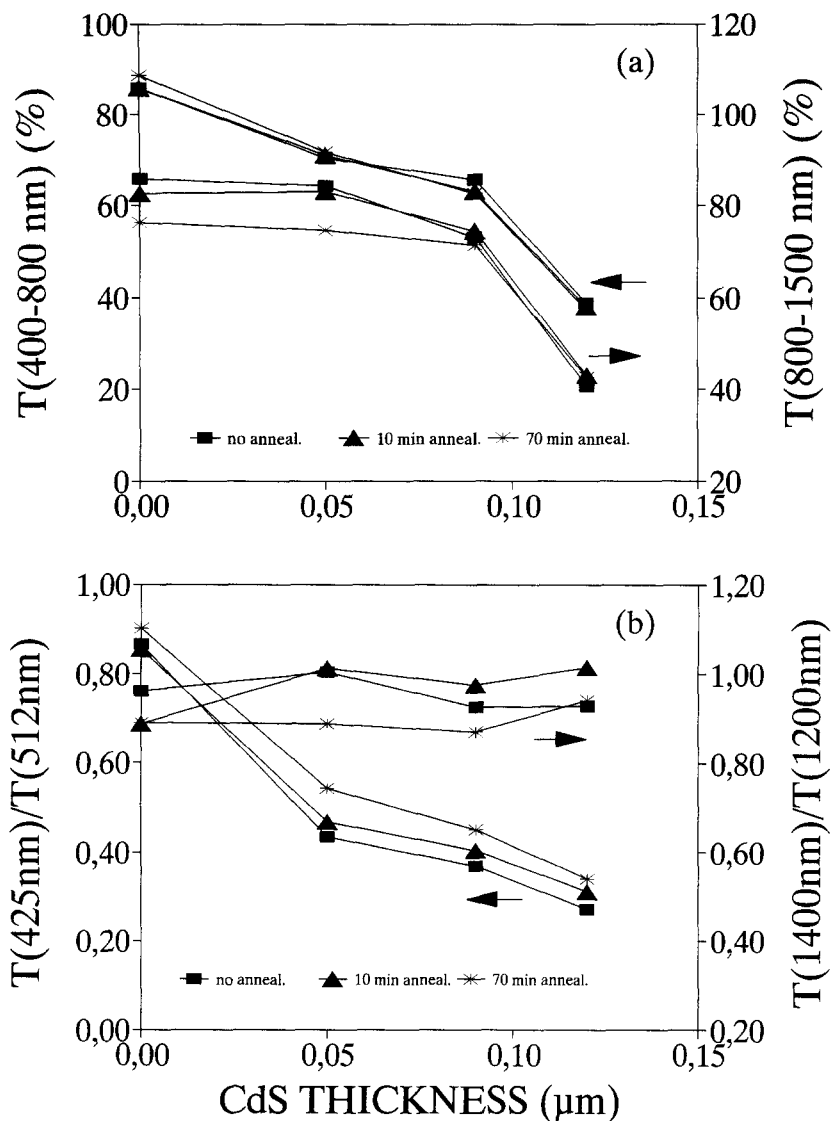


Fig. 10. Influence of the 200°C air annealing time on the (a) visible and infrared average transmissions and (b) $T_{425 \text{ nm}}/T_{512 \text{ nm}}$ and $T_{1400 \text{ nm}}/T_{1200 \text{ nm}}$ ratios for room-temperature ITO films made on CdS substrates of various thicknesses.

Fig. 9, since the oxygen has filled the oxygen vacancies and, therefore, its conductivity has been reduced. The optical properties of the CdS-ITO samples, see Fig. 10, especially the average transmittances in the infrared region (Fig. 10a) are again better than those of the CdS-ZnO films. The evolution of the ITO-based coatings with the several air heating times has been summarised in Table 1.

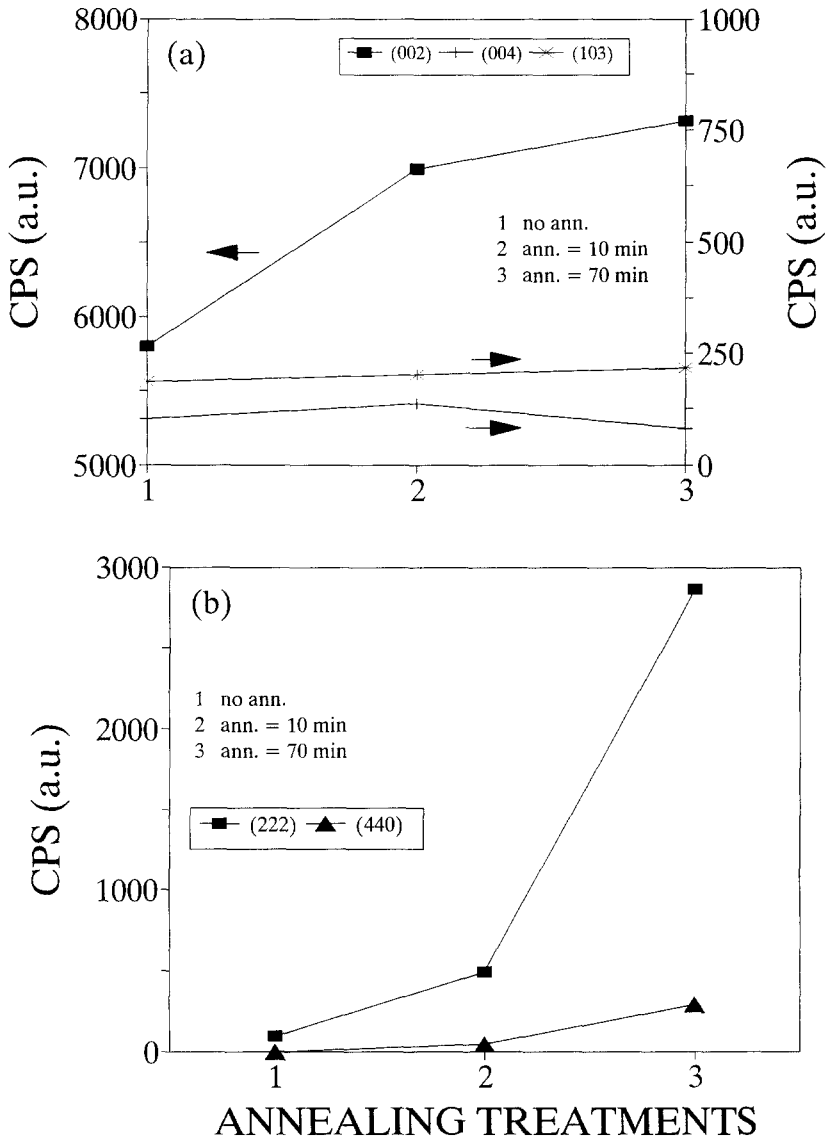


Fig. 11. Evolution of the X-ray diffraction peaks with the 200°C air annealing time for samples prepared with $d_{\text{CdS}} = 0.05 \mu\text{m}$ and (a) ZnO and (b) ITO.

The investigation of the structural properties has evidenced a TCO crystallinity improvement with the annealing time. As can be seen in Fig. 11, the (002) ZnO (Fig. 11a) and the (222) ITO (Fig. 11b) X-ray diffraction peaks have raised with the 200°C air annealing. Nevertheless, since the optimisation of the CuInSe₂-based solar cells is induced by heating in air for short times not longer that 10 minutes, and taking into account that the present results have indicated that 70-minute air annealing does not

improve the optoelectronic features of the window layers, it has been concluded that a 10-minute air heat treatment at 200°C is optimum not only for enhancing the absorber photovoltaic response but also for improving the crystalline structure of the window maintaining its electro-optical quality invariable.

4. Conclusions

Window coatings consisting on chemical bath deposited cadmium sulphide and rf-magnetron sputtered indium tin oxide or aluminium-doped zinc oxide have been optimised for being applied in CuInSe₂ and CdTe-based photovoltaic solar cells. Different CdS thicknesses have been tested. It has been concluded that the use of cadmium sulphide films thinner than 0.1 μm is necessary in order to avoid important optical absorption losses and conductivity deterioration. Although both types of CdS–TCO bilayers ($d_{\text{CdS}} < 0.1 \mu\text{m}$) have shown good optoelectronic, morphological and structural characteristics at 25 and 200°C substrate temperature, ITO-based samples have a higher infrared transmission than ZnO-based films do.

Considering that CuInSe₂-based devices improve after air-annealing, two air heat treatments have been carried out at 200°C for 10 and 70 minutes on bilayers made at room-temperature. The shorter annealings have resulted to be optimum in order to improve crystalline structure maintaining electro-optical quality invariable.

Acknowledgements

This work has been supported by the Spanish Ministry of Industry and Energy through CIEMAT-IER, the CICYT Project MAT-94-1270-CE, the CAM Project 103/92 and the CEC-Joule Program JOU-CT-92-0141.

References

- [1] T.L. Chu, S.S. Chu, C. Ferekides, C.Q. Wu, J. Britt and C. Wang, *J. Appl. Phys.* 70 (1991) 7608.
- [2] J.Hedström, H. Olsen, M. Bodegård, A. Kylner, L. Stolt, D. Harisko, M. Ruckh and H.W. Schock, 23rd IEEE Photovoltaic Specialists Conf., Louisville, 1993, p. 364.
- [3] J.M. Doña, Doctoral Thesis, Universidad Autónoma de Madrid, 1995.
- [4] N. Romeo, A. Bosio and V. Canevari, *Solar Cells* 22 (1987) 23.
- [5] H. Higuchi, T. Arita, T. Aramoto, T. Nishio, K. Hiramatsu, A. Hanafusa, N. Ueno, K. Omura, N. Nakayama, H. Takakura and M. Murozono, 23rd IEEE Photovoltaic Specialists Conf., Louisville, 1993, p. 409.
- [6] R.W. Buckley, B. Cotier, K. Dixon, T. Gallager and N. Goddard, 10th European Photovoltaic Solar Energy Conf., Lisbon, 1991, p. 584.
- [7] F. Tepehan and N. Özer, *Sol. Energy Mater. Sol. Cells* 30 (1993) 353.
- [8] H.D. Kim, D.S. Kim, K. Cho, B.T. Ahn and H.B. Im, *J. Electrochem. Soc.* 141 (1994) 3572.
- [9] R. Arya, J. Fogleboch, T. Lommasson, R. Podlesny, L. Russell, S. Skibo, S. Wiedeman, A. Rothwarf and R. Birkmire, NREL TIP-413-5759/DE 93018223.

- [10] L. Russell, B. Fieselmann and R.R. Arya, 23rd IEEE Photovoltaic Specialists Conf., Louisville, 1993, p. 581.
- [11] J.M. Doña and J. Herrero, *J. Electrochem. Soc.* 139 (1992) 2810.
- [12] J.M. Doña and J. Herrero, 6th Int. Photovoltaic Science and Engineering Conf., New Delhi, 1992, p. 985.
- [13] M.A. Martínez, J. Herrero and M.T. Gutiérrez, *Thin Solid Films* 269 (1995) 80.
- [14] M.A. Martínez, J. Herrero and M.T. Gutiérrez, *Sol. Energy Mater. Sol. Cells* 31 (1994) 489.
- [15] M.A. Martínez, J. Herrero and M.T. Gutiérrez, to be published in *Sol. Energy Mater. Sol. Cells*.
- [16] T. Negami, M. Nishitani, T. Wada and T. Hirao, 11th European Photovoltaic Solar Energy Conf., Montreux, 1992, p. 783.
- [17] R.A. Sasala and J.R. Sites, *Solar Cells* 30 (1991) 101.
- [18] A.M. Goodman, *Appl. Opt.* 17 (1978) 2779.
- [19] D. Lincot and R.O. Borges, *J. Electrochem Soc.* 139 (1992) 1880.
- [20] ASTM card n° 6-0314.
- [21] ASTM card n° 6-416.
- [22] ASTM card n° 5-664.